A Geometrical Framework for Quantum Incompatibility Resources

Xiaolin Zhang,[1] Rui Qu,[1] Zehong Chang,[1] Quan Quan,[1] Hong Gao,[1] Fuli Li,[1] and Pei Zhang[1,*]

[1] *Ministry of Education Key Laboratory for Nonequilibrium Synthesis and Modulation of Condensed Matter, Shaanxi Province Key Laboratory of Quantum Information and Quantum Optoelectronic Devices, School of Physics, Xi'an Jiaotong University, Xi'an 710049, China*

(Dated: August 5, 2021)

Quantum incompatibility is a fundamental property in quantum physics and is considered as a resource in quantum information processing tasks. Here we construct a framework based on the nonlinear incompatibility witness originated from the guessing probability gap to describe the incompatibility processes of two noisy mutually unbiased bases. The incompatibility witness is originated from convex combinations of partitioned ensembles via quantum state discrimination tasks. Moreover, the framework provides geometrical vectors to describe incompatibility processes. In this framework, we define the degree of quantum incompatibility which is associated with geometrical information and apply the quantifier to evaluate incompatibility between two noisy mutually unbiased base ensembles. Finally, we demonstrate that the degree of incompatibility capture the resource of incompatibility. This geometrical framework gives the evidence that vectors can be utilized to describe resourceful incompatibility and may help explore geometrical features of quantum resources.

I. INTRODUCTION

Quantum incompatibility is a fundamental property in quantum physics, which is quite different from classical physics that some observables or measurements cannot commute with each other and implies that we cannot acquire precise information from them simultaneously. Quantum incompatibility is considered as an important resource for quantum phenomena and information processing, including quantum nonlocality [1], measurement uncertainty relations [2, 3], uncertain relation [3], contextuality [4, 5], and quantum steering [6–8]. Therefore, it is important to witness and quantify quantum incompatibility as a resource for developing quantum applications.

In order to detect incompatibility, some methods based on entanglement schemes [2, 9–11] have been proposed. In these entanglement-based schemes, a quantum entanglement source and spacelike separation are required. Fortunately, entanglement is confirmed not necessarily needed for quantum incompatibility features, which provides an alternative for detecting quantum incompatibility. Recently quantum state discrimination (QSD) tasks have been applied in witnessing quantum incompatibility [7, 12–14].

QSD can be applied to detect quantum coherence [15, 16], entropic uncertainty relations, accessible information [16, 17]. Moreover, quantum incompatibility can always be detected by a QSD task with partitioned intermediate information [12]. In a two-party QSD scenario [18–20], Alice chooses one state from two disjoint state ensembles and announces the information of the chosen ensemble to Bob. Then Bob can decide to perform his measurement either before or after Alice's announcement. As a result, he can have a higher guessing probability hearing the prior information compared to post-measurement information. The gap between the guessing probabilities can be a witness of incompatibility and the robustness of incompatibility is an advantageous quantifier of quantum incompatibility [13, 15, 16, 21–24].

In order to investigate incompatibility witnesses quantificationally, it is convenient to prepare two disjoint state ensembles as two sets of mutually unbiased bases (MUBs) under different noise levels. MUB measurements are among of the most representative incompatible measurements and have been applied in many quantum information protocols [25, 26]. Two families of orthonormal bases $\left\{\psi_i^A\right\}_{i=0}^{d-1}$ and $\left\{\phi_j^B\right\}_{j=0}^{d-1}$ of a d-dimensional Hilbert space $\mathcal{H}_d$ are said to be mutually unbiased if, for any i, j, $\left|\left\langle\psi_i^A \mid \phi_j^B\right\rangle\right|^2=\frac{1}{d}\left(1-\delta_{AB}\right)+\delta_{AB}\delta_{ij}$ [27].

Recently, incompatibility witnesses based on hyperplanes have been established [12], linear incompatibility witnesses (LIWs) have been verified [14] and the robustness of incompatibility has been proposed [7], which quantifies the quantum incompatibility with the robustness to noises. However, there still exists a question of how to utilize the quantum incompatibility resource, which indicates a need for a framework to describe quantum incompatibility processes.

In this paper, we construct a geometrical framework for quantum incompatibility processes based on the gap of prior- and post-measurement guessing probabilities in a two-part QSD scenario. In the framework, we define inner incompatibility between two ensembles and general incompatibility for practical QSD tasks. Furthermore, the degree of incompatibility is defined to quantify the quantum incompatibility resource and can be linearly mapped to geometrical properties in the convex model which is intrinsically originated from convex combination of two noisy MUB ensembles. Finally, we apply the framework to inner incompatibility to show its advantages in describing incompatibility and associate the degree with quantum resources.

* zhangpei@mail.ustc.edu.cn

II. NONLINEAR WITNESS CONSTRUCTION VIA QUANTUM STATE DISCRIMINATION TASKS

A. Quantum State Discrimination

Consider a pair of POVMs A and B labeled $A = A_x$ and $B = B_y$, satisfying $\Sigma_x A_x = \mathbb{I}$ and $\Sigma_y B_y = \mathbb{I}$ with outcomes x and y, respectively. A and B are compatible if there exists a joint or parent POVM $J_{x,y}$ satisfying $\Sigma_y J_{x,y} = A_x$ and $\Sigma_x J_{x,y} = B_y$. A pair of arbitrary POVMs can be observed by two noisy MUBs and result in respective particular probability distributions.

In a two-party QSD scenario, Alice prepares two ensembles of quantum states $\mathcal{E}_X = \{p(x), \Psi_x\}_x$ and $\mathcal{E}_Y = \{p(y), \Phi_y\}_y$, where $p(x)$ and $p(y)$ are the probability distributions of POVMs A and B, respectively. Then Bob receives a merged ensemble $\mathcal{E}$ with a proportion parameter q as follows:

$$\begin{aligned}\mathcal{E} &= q\mathcal{E}_X + (1-q)\mathcal{E}_Y \\ &= \{qp(x), \Psi_x; (1-q)p(y), \Phi_y\}_{x,y} \\ q &\in (0,1].\end{aligned} \tag{1}$$

Bob has two strategies to guess the state sent from Alice. If the information of given ensemble $\mathcal{E}_X$ or $\mathcal{E}_Y$ is announced before the measurement, the guesser Bob will perform corresponding measurement M or N to detect the state from ensembles $\mathcal{E}_X$ or $\mathcal{E}_Y$, respectively. The guessing probability for one ensemble observed is $P_{\text{guess}}(\mathcal{E}_X; M) = \sum_x p(x) \operatorname{Tr}(M_x \Psi_x)$. Then the total guessing probability with prior information can be written out as follows:

$$\begin{aligned}P_{\text{guess}}^{\text{prior}}(\mathcal{E}; M, N) =& qP_{\text{guess}}(\mathcal{E}_X; M) \\ &+ (1-q)P_{\text{guess}}(\mathcal{E}_Y; N).\end{aligned} \tag{2}$$

In contrast, if the information of the given set $\mathcal{E}_X$ or $\mathcal{E}_Y$ is announced after the measurement, Bob has to use a joint measurement $J(A,B)$ to guess the state labeled with a cartesian product (X,Y) which is the outcome of MUB measurements, and adjusts $J(A,B)$ after each round to match the optimal joint measurement. Then the post information guessing probability can be written as follows:

$$P_{\text{guess}}^{\text{post}}(\mathcal{E}) = \max_J P_{\text{guess}}(\mathcal{E}; J). \tag{3}$$

If POVMs A and B are compatible, their observation (X,Y) will be devided into compatible pairs $\mathcal{O}_{X,Y}^{\text{com}}$, else into the incompatible pairs $\mathcal{O}_{X,Y}^{\text{inc}} \equiv \overline{\mathcal{O}_{X,Y}^{\text{com}}}$. It has been proven that for incompatible measurements, there always exists a partitioned state ensemble $\mathcal{E}$ such that $P_{\text{guess}}^{\text{post}}(\mathcal{E}) < P_{\text{guess}}^{\text{prior}}(\mathcal{E}; M, N)$. Hence the incompatibility witnesses separating $\mathcal{O}_{X,Y}^{\text{com}}$ and $\mathcal{O}_{X,Y}^{\text{inc}}$ in the form of hyperplanes can be written as follows [12]:

$$W = P_{\text{guess}}^{\text{post}}(\mathcal{E}) - P_{\text{guess}}^{\text{prior}}(\mathcal{E}; M, N). \tag{4}$$

B. Incompatibility Witnesses Based on Noisy MUBs

Here, we explore the incompatibility of d-dimension ensembles $(\mathcal{E}_X, \mathcal{E}_Y)$ with noises:

$$\begin{aligned}&\mathcal{E}_X : \left\{\frac{1}{d}, r_x \left|\psi_i^A\right\rangle \left\langle\psi_i^A\right| + (1-r_x)\,\mathbb{I}/d\right\}_i \\ &\mathcal{E}_Y : \left\{\frac{1}{d}, r_y \left|\phi_j^B\right\rangle \left\langle\phi_j^B\right| + (1-r_y)\,\mathbb{I}/d\right\}_j \\ &i,j \in (1,2,\cdots,d), (r_x, r_y) \in ((0,1],(0,1]).\end{aligned} \tag{5}$$

Parameters r_x and r_y represent the sharpness of different state ensembles, and the corresponding measurements performed by Bob are MUB measurements under different noise level parameters s_x and s_y:

$$\begin{aligned}&M : \left\{s_x \left|\psi_i^A\right\rangle \left\langle\psi_i^A\right| + (1-s_x)\,\mathbb{I}/d\right\}_i \\ &N : \left\{s_y \left|\phi_j^B\right\rangle \left\langle\phi_j^B\right| + (1-s_y)\,\mathbb{I}/d\right\}_j \\ &i,j \in (1,2,\cdots,d), (s_x, s_y) \in ((0,1],(0,1]).\end{aligned} \tag{6}$$

In this QSD task, we set a balanced portional parameter $q = \frac{1}{2}$ and the optimal joint measurement $J(A,B)$ for a pair of MUBs is given in Ref. [28]:

$$\begin{aligned}J_{i,j} =& b(r_x|\psi_i\rangle\langle\psi_i| + r_y|\phi_j\rangle\langle\phi_j|) - \frac{dc}{d-1}(|\psi_i\rangle\langle\psi_i| + \\ & |\phi_j\rangle\langle\phi_j| - |\psi_i\rangle\langle\psi_i||\phi_j\rangle\langle\phi_j| - |\phi_j\rangle\langle\phi_j||\psi_i\rangle\langle\psi_i|) \\ b =& \frac{1}{\sqrt{r_x^2 + r_y^2 - \frac{2d-4}{d}r_x r_y}} \\ c =& \frac{1}{2}\left(\frac{r_x + r_y}{\sqrt{r_x^2 + r_y^2 - \frac{2d-4}{d}r_x r_y}} - 1\right),\end{aligned} \tag{7}$$

where d is the dimension of MUBs.

Here, we can give the mathematical forms of $P_{\text{guess}}^{\text{post}}$ and $P_{\text{guess}}^{\text{prior}}$, which are detailed in Appendix A 1:

$$\begin{aligned}P_{\text{guess}}^{\text{post}} =& \frac{1}{4}\sqrt{r_x^2 + r_y^2 - \frac{2d-4}{d}r_x r_y} \\ &+ \frac{d-2}{4d}(r_x + r_y) + \frac{1}{d} \\ P_{\text{guess}}^{\text{prior}} =& \frac{d-1}{2d}(r_x s_x + r_y s_y) + \frac{1}{d}.\end{aligned} \tag{8}$$

Combining Eq. (8) and Eq. (4), we can write out the

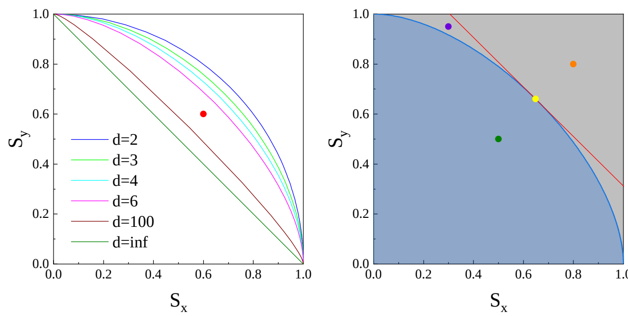

FIG. 1. The witnesses for serval dimensions have been shown as convex curves and the cases for the incompatibility witness are discussed. (a) The cases $d = 2, 3, 4, 6, 100$ and ∞. The curves of the boundary for $W = 0$ are ellipses. The case $d = 2$ and $d = \infty$ are special, which are a quadrant and line, respectively. The red point is compatible in the case $d = 6$, but incompatible in the case $d = 100$. (b) There cases for the incompatibility witness. In the case $d = 5$, the yellow point and red line are tangent point and its tangent line. There are three cases in incompatibility witnesses: olive point: inside the curve; purple: outside the curve but inside the line; orange point: outside the line.

witness of varibles (s_x, s_y) with parameters (r_x, r_y):

$$W = \frac{1}{4}\sqrt{r_x^2 + r_y^2 - \frac{2d-4}{d} r_x r_y} + \frac{d-2}{4d}(r_x + r_y) - \frac{d-1}{2d}\left(r_x s_x + r_y s_y\right). \tag{9}$$

Obviously, this function is a nonlinear witness of (r_x, r_y, s_x, s_y). And when parameters (r_x, r_y) are fixed, the function will become a linear function for (s_x, s_y), which is the form of linear witnesses corresponding to the hyperplanes separating $\mathcal{O}^{\rm com}_{X,Y}$ and $\mathcal{O}^{\rm inc}_{X,Y}$ [14].

Then we discuss the properties of dimensions for the boundary curve in Fig. 1. Intuitively, when the dimension increases, the incompatibility between two MUBs also increases [29]. When the dimension is infinity, the curve approaches a line, which implies the convex combination of incompatible measurements approaches a linear combination of incompatibility.

There are three possible cases in practical QSD scenario in Fig. 1.

1. $W < 0$: Incompatibility is detected existent for this four parameters (r_x, r_y, s_x, s_y), which corresponds to the orange point in Fig. 1.

2. $W = 0$: $P^{\rm post}_{\rm guess} = P^{\rm prior}_{\rm guess}$, which is the boundary between compatibility and incompatibility.

3. $W > 0$: Compatibility is detected existent even though the joint measurement performed is not optimal, which corresponds to the olive and purple points in Fig. 1.

In conclusion, we have discussed the properties of nonlinear incompatibility witness (NLIW) with four parameters (r_x, r_y, s_x, s_y) in the language of geometry. The boundary between compatibility and incompatibility for all noisy MUBs labeled with (r_x, r_y) can be represented as a two-dimension convex curve, which implies geometrical properties in the model originated from incompatibility witnesses. Here, we name the model for convex model because the model is essentially originated from the convex combination of partitioned information. In the following contents, we will inspect the model and define a more intuitive framework for its geometrical properties.

III. THE GEOMETRICAL FRAMEWORK FOR QUANTUM INCOMPATIBILITY

A. Defination of Inner Incompatibility

In practical scenario, the function of NLIW has four parameters (r_x, r_y, s_x, s_y) and they four are mutually independent of others. Intuitively, the incompatibility between two ensembles labeled with (r_x, r_y) is not relevant to (s_x, s_y), and if $(s_x, s_y) = (1, 1)$, the solution of NLIW does not exist, which means the incompatibility phenomenon always exists even if we reduce (r_x, r_y) to a low value. Sensibly, two noisy ensembles can be compatible as the weight of white noise gradually increases to a critical point.

Thus, we define the inner incompatibility between two ensembles (r_x, r_y) by fixing $(r_x, r_y, s_x = r_x, s_y = r_y)$. This defination implies that measure an ensemble with its equal measurement, which actually evaluates the two ensembles' ability to maintain their fidelity and compares it with the observation of their optimal joint measurement. Then the NLIW is only a function of (r_x, r_y) which has solutions for compatibility. For example, two ensembles labeled with $(r_x = 0.1, r_y = 0.1)$ are compatible.

When $(s_x \neq r_x, s_y \neq r_y)$, measurements performed by Bob are independent from ensembles sent from Alice, a more general framework of quantum incompatibility is needed to investigate more universal cases of QSD tasks. In the following contents, we will define the framework for general incompatibility and recall inner incompatibility after constructing the general incompatibility framework.

B. Defination of General Incompatibility

In the case that four parameters (r_x, r_y, s_x, s_y) can be adjusted independently, it is necessary for the four parameters to have a unified explanation. Here, we define general incompatibility as a general description of incompatibility in the QSD scenario. Recalling Eq. (5), the MUB part in ensembles represents incompatibility and white noise represents compatibility. Recalling Eq. (6), the MUB part in measurements represents extracting incompatibility from ensembles and white noise represents no operation with outcomes of average probability distributions. In conclusion, (r_x, r_y) labels ensembles and (s_x, s_y) scales the incompatibility.

It's worth noting that the operators in Eq. (6) are positive if and only if $(s_x, s_y) \in ([\frac{1}{1-d}, 1], [\frac{1}{1-d}, 1])$ [12], while in the general incompatibility framework, we restrict them to positive values $(s_x, s_y) \in ((0,1], (0,1])$ as noisy versions of the sharp measurements [30].

C. Geometrical Properties of General Incompatibility in Convex Model

In Fig. 1, an arbitrary fixed (r_x, r_y) corresponds to a fixed hyperplane, and all (r_x, r_y) is supposed to draw corresponding hyperplanes which together form the convex curve. Therefore, we can write out the coordinate of the point on the broundary curve, which is detailed in Appendix A 2:

$$\begin{aligned} s_x &= \frac{1}{2(d-1)}[\frac{dk-(d-2)}{\sqrt{k^2+1-\frac{2d-4}{d}k}} + (d-2)] \\ s_y &= \frac{1}{2(d-1)}[\frac{d-(d-2)k}{\sqrt{k^2+1-\frac{2d-4}{d}k}} + (d-2)] \\ k &= \frac{r_x}{r_y}. \end{aligned} \tag{10}$$

It is interesting that the curve is a function of k and not directly relevant to the value of (r_x, r_y). Obviously, a set of (s_x, s_y) can be described by a point in the cartesian coordinate system, while a set of (r_x, r_y) corresponds to a k which can also be seen as a point (s_{x_0}, s_{y_0}) on the curve. The transformation implies the optimal joint measurement can be replaced by two equivalent portional submeasurements (s_x, s_y) geometrically. Then the post-measurement guessing probability can be replaced by a point on the convex curve as $P^{Post} = P(s_{x_0}, s_{y_0})$ with (s_{x_0}, s_{y_0}) satisfying Eq. (10). What's more, the prior-measurement guessing probability of portional measurements can replaced by a point (s_x, s_y) as $P^{Prior} = P(s_x, s_y)$. As a result, the four parameters are unified as points in the geometrical curve model.

D. The Defination of The Degree of Incompatibility

The degree of incompatibility has been charactered by the robustness of incompatibility and confirmed as a quantifier of incompatibility resources [7]. However, the geometrical property for four parameters disappears because the robustness is defined as the ability of the system to resist noises, which eliminates interaction information among the four parameters. Therefore, we start to construct a new defination of the degree of incompatibility in the QSD scenario. The new defination has two desirable properties:

1. It is related or mapped to the geometrical property of the convex model.

2. It is relevant to the sharpness of ensembles and geometrical distance in the convex model, for example $D = S \times m, \quad m = r_x + r_y$.

In Fig. 2, (s_x, s_y) and (s_{x_0}, s_{y_0}) represent prior- and post-measurement guessing probabilities, respectively. If there exists a new defination of the degree of incompatibility as D, we hope D can satisfy $D \propto P(s_x - s_{x_0}, s_y - s_{y_0})$. In this way, we can convert D into a geometrical vector in a two-dimension cartesian coordinate system. Fortunately, considering Eq. (10), it is convenient to construct D satisfying the two requests above:

$$\begin{aligned} D(r_x, r_y, s_x, s_y) &= P^{Prior} - P^{Post} \\ &= \frac{d-1}{2d}\left[r_x\left(s_x - s_{x_0}\right) + r_y\left(s_y - s_{y_0}\right)\right] \\ &= \frac{d-1}{2d}\left[r_x\Delta_x + r_y\Delta_y\right]. \end{aligned} \tag{11}$$

We call Eq. (11) the vector form of D. In Fig. 2, (Δ_x, Δ_y) represents the vector from P^{Post} to P^{Prior}. Here we construct a linear map from geometrical space to the degree D with coefficients associated with (r_x, r_y) and the dimension d. Moreover, using this form, we can compare different (s_x, s_y) under a common given ensembles (r_x, r_y) by a vector from (s_x, s_y) to (s_{x_1}, s_{y_1}). In addition, if (s_x, s_y) is exactly at the special point (s_{x_0}, s_{y_0}), there appears an interesting phenomenon that as long as (r_x, r_y) maintain its ratio k fixed, compatibility always exists.

Further more, the length of D can be given as

$$D = \frac{d-1}{2d}\sqrt{r_x^2 + r_y^2} \times h. \tag{12}$$

We call Eq. (12) the distance form of D. In Fig. 2, h represents the vertical distance from the tangent line of (s_{x_0}, s_{y_0}) to measurements (s_x, s_y). The tangent line is actually the LIW with a fixed (r_x, r_y), and the direction of h represents whether it is incompatible or not. The value $|h|$ can also be linearly mapped into the degree D with a coefficient related to the sharpness of ensembles. Obviously, all points on one parallel of the tangent line have a common D, which implies that different (s_x, s_y) can achieve the same observation. Similiarly, the tangent line of (s_{x_0}, s_{y_0}) is the special line where all points on the line are compatible as long as (r_x, r_y) maintains a fixed ratio k.

In Fig. 2, the region inside convex curve for (s_x, s_y) represents the observation is compatible regadless of ensemble sharpness (r_x, r_y), because no matter what k is, (s_x, s_y) is always inside the linear witness. But if (s_x, s_y)

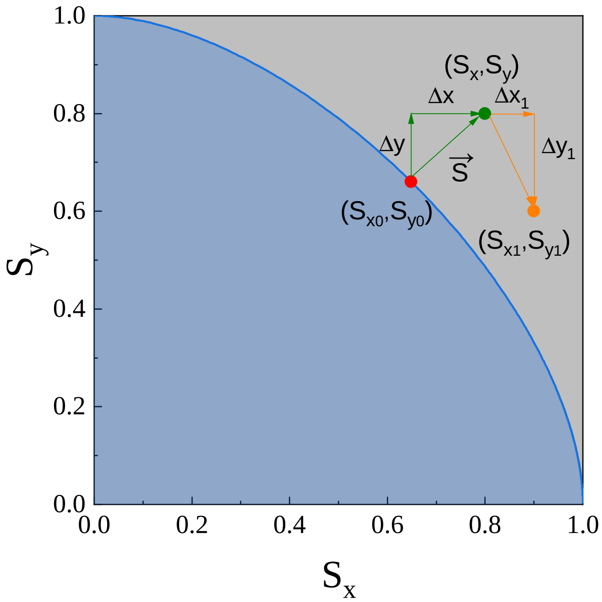

(a) vector form

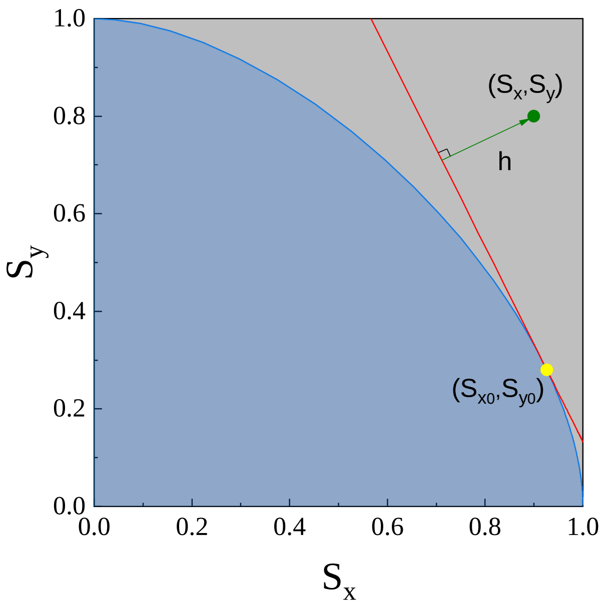

(b) distance form

FIG. 2. The newly defined D has two forms as Eq. (11) and Eq. (12). (a) The vector form of D is an effective tool to describe incompatibility by vector connecting equivalent optimal joint measurement (s_{x_0}, s_{y_0}) and submeasurements (s_x, s_y), which is also able to describe incompatibility between different measurements (s_x, s_y) and (s_{x1}, s_{y1}) in the case of (r_x, r_y) fixed. S represents geometrical distance. (b) The distance form of D is a more intuitive tool to describe incompatibility by distance h between measurements implemented and linear witnesses. All measurements on the parallel of one linear witness have the same degree of incompatibility.

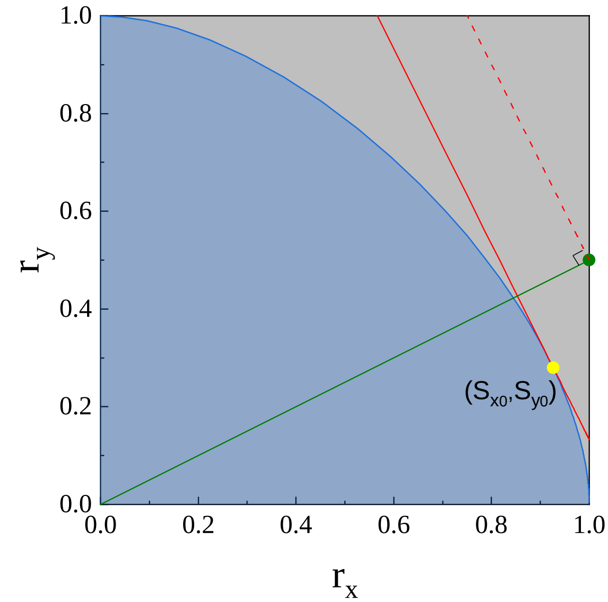

FIG. 3. In the case of inner incompatibility, D can be worked out only using information from the picture, which is an effective and intuitive tool to detect and quantify incompatibility of a pair of ensembles. The olive line connects the $(0, 0)$ and (r_x, r_y). The red line and its parallel represent LIW and they are vertical to the olive line.

is in the region outside the convex curve, the specific question about whether incompatible or not should be considered as two cases of purple and orange points in Fig. 1.

E. Application of General Incompatibility in Inner Incompatibility

The general incompatibility framework provides an excellent model to describe inner incompatibility phenomena in Fig. 3. We can prove that the line connecting (r_x, r_y) and $(0, 0)$ is exactly vertical to the corresponding tangent line, which is the LIW of (r_x, r_y). If a pair of ensembles labeled with (r_x, r_y) is given, we can obtain its equivalent optimal joint measurement (s_{x_0}, s_{y_0}) and D via the following steps. Firstly, We need to draw a line connecting (r_x, r_y) and $(0, 0)$ and draw parallels of its vertical lines. And then, if we find one parallel which is tangent to the convex curve, it is exactly the LIW of (r_x, r_y), and the tangent point will be the equivalent optimal joint measurement (s_{x_0}, s_{y_0}). Finally, the degree of incompatibility D can be obtained via the linear map from (r_x, r_y), h and d.

F. The Geometrical Framework for Quantum Incompatibility Resources

There are 3 main ingredients for a resource theory [31]:

1. a set of free or resourceless objects.

2. a set of expensive or resourceful objects.

3. a set of allowed transformations between objects, which is supposed unable to create resourceful objects from resourceless objects.

In the geometrical framework, compatible pairs of measurements correspond to the resourceless objects and incompatible pairs correspond to resourceful objects. Then, considering two forms of D, paths of vectors in the convex model carry the information of transformations of quantum incompatibility resources and are linearly mapped into the degree of incompatibility as a quantifier of incompatibility resources.

Obviously, for quantum incompatibility resources in practical QSD tasks, namely general incompatibility, the quantifier D decreases when sharpness (r_x, r_y) declines maintaining a fixed ratio $k = \frac{r_x}{r_y}$. Moreover, for quantum incompatibility between two ensembles, namely inner incompatibility, when (r_x, r_y) descreases and drops inside the convex curve, the pair of ensembles (r_x, r_y) is compatible and resourceless, which implies the transformation from expensive objects to free objects which is not able to observe incompatibility phenomena between resourceless objects. It can be seen that D satisfies the three ingredients, and captures the resource of incompatibility.

This advantage of the new framework as a geometrical model is different from the robustness of incompatibility, but they can be linearly correlated with each other in QSD tasks. The robustness of incompatibility in the QSD scenario can be as follows:

$$1 + R(A, B) \geq \frac{P^{Prior}}{P^{Post}}. \tag{13}$$

D can be proven portional to the lower bound of R in the case of fixed (r_x, r_y) [7, 14].

IV. CONCLUSION

We construct a geometrical framework for quantum incompatibility resources that provides vectors to carry information of transformations for resources. It is also advantageous in describing the incompatibility phenomena geometrically in practical QSD tasks. We have shown that for incompatible measurements, it is feasible to detect and quantify incompatibility under noisy MUBs with vectors. In this frame, the geometrical properties in the convex model can be linearly mapped to the degree of incompatibility as a resource and thus the incompatibility process tasks are able to be operated intuitively with corresponding vectors. Moreover, these properties can be verified by QSD experiments requiring no entanglement.

Our characterization yields a geometrical interpretation of incompatibility resources in QSD tasks: the operations with path information and the degree of incompatibility can be described with geometrical vectors. The degree of incompatibility D is demonstrated as a quantifier of incompatibility resource, which may have potential in other quantum information processes.

Einstein-Podolsky-Rosen steering is related to quantum incompatibility and able to be described in QSD tasks. If two ensembles are compatible, there must exist a local-hidden-state model which implies no steering. And every set of incompatible measurements has the potential of generating EPR steering [7, 32, 33]. These modifications will be an interesting matter of investigation in the case of incompatibility witnesses.

ACKNOWLEDGMENTS

This work was supported by the National Nature Science Foundation of China (Grants No. 11534008, 11804271 and 91736104), Ministry of Science and Technology of China (2016YFA0301404), and China Postdoctoral Science Foundation via Project No. 2020M673366.

Appendix A: THEORETICAL DETAILS

1. Prior- and post-measurement guessing probability

In the two-party system, we have four MUBs labeled with (r_x, r_y, s_x, s_y) defined in Eq. (5) and Eq. (6). We set the portional parameter $q = \frac{1}{2}$ and mean probability distribution $p(x) = p(y) = \frac{1}{d}$:

$$\begin{aligned}
P_{guess}^{prior} &= \frac{1}{2} P_{guess}(\mathcal{E}_X; M) + \frac{1}{2} P_{guess}(\mathcal{E}_Y; N) \\
&= \frac{1}{2} \sum_x p(x) \operatorname{Tr}(M_i (r_x |\psi_i^A\rangle\langle\psi_i^A| + (1 - r_x)\mathbb{I}/d)) \\
&+ \frac{1}{2} \sum_y p(y) \operatorname{Tr}(N_j (r_y |\phi_j^B\rangle\langle\psi_j^B| + (1 - r_y)\mathbb{I}/d)) \\
&= \frac{1}{2}(r_x s_x + \frac{s_x + r_x - 2r_x s_x}{d} + \frac{1 - s_x - r_x + r_x s_x}{d}) \\
&+ \frac{1}{2}(r_y s_y + \frac{s_y + r_y - 2r_y s_y}{d} + \frac{1 - s_y - r_y + r_y s_y}{d}) \\
&= \frac{d-1}{2d} (r_x s_x + r_y s_y) + \frac{1}{d}.
\end{aligned} \tag{A1}$$

We recall Eq. (7), and write the result as follows:

$$
\begin{aligned}
P_{guess}^{post} &= P_{guess}(\mathcal{E}; J) \\
&= \sum_{i,j} p(x)p(y)\,\mathrm{Tr}((\frac{1}{2}\Psi_x + \frac{1}{2}\Phi_y)J_{i,j}) \\
&= \frac{1}{2}\,\mathrm{Tr}(J_{i,j}(r_x|\psi_i^A\rangle\langle\psi_i^A| + (1-r_x)\mathbb{I}/d)) \\
&+ \frac{1}{2}\,\mathrm{Tr}(J_{i,j}(r_y|\phi_j^B\rangle\langle\phi_j^B| + (1-r_y)\mathbb{I}/d)) \\
&= \frac{1}{2}\,\mathrm{Tr}(J_{i,j}(r_x|\psi_i^A\rangle\langle\psi_i^A|) \\
&+ \frac{1}{2}\,\mathrm{Tr}(J_{i,j}(r_y|\phi_j^B\rangle\langle\phi_j^B|) \\
&+ \frac{1}{2}\,\mathrm{Tr}(J_{i,j}((2-r_x-r_y)\mathbb{I}/d) \\
&= \frac{r_x}{2}(b(r_x + \frac{r_y}{d}) - c) + \frac{r_y}{2}(b(r_y + \frac{r_x}{d}) - c) \\
&+ \frac{2-r_x-r_y}{d}(b-2c) \\
&= \frac{1}{4}\sqrt{r_x^2 + r_y^2 - \frac{2d-4}{d}r_x r_y} + \frac{d-2}{4d}(r_x+r_y) + \frac{1}{d}.
\end{aligned}
\tag{A2}
$$

If we set $d = 3$ and $(s_x, s_y) = (1, 1)$, the results both accord with the experiment result in Ref. [14].

2. Points on the boundary curve

Exploring the geometrical properties in the case of $W = 0$ in Eq. 9, we have:

$$
\begin{aligned}
\frac{d-1}{2d}(r_x s_x + r_y s_y) = \frac{1}{4}\sqrt{r_x^2 + r_y^2 - \frac{2d-4}{d}r_x r_y} \\
+ \frac{d-2}{4d}(r_x + r_y).
\end{aligned}
\tag{A3}
$$

Obviously, it is a function of a straight line for (s_x, s_y), and if we set $k = \frac{r_x}{r_y}$, we will obtain a new form:

$$
\frac{d-1}{2d}(ks_x + s_y) = \frac{1}{4}\sqrt{k^2 + 1 - \frac{2d-4}{d}k} + \frac{d-2}{4d}(k+1).
\tag{A4}
$$

We utilize the intersection of two nearby lines to simulate the boundary curve, and when the variation of k between two lines is small enough, we have:

$$
\begin{aligned}
s_x &= \frac{2d}{d-1}\frac{\partial(\frac{1}{4}\sqrt{k^2+1-\frac{2d-4}{d}k} + \frac{d-2}{4d}(k+1))}{\partial k} \\
&= \frac{1}{2(d-1)}[\frac{dk-(d-2)}{\sqrt{k^2+1-\frac{2d-4}{d}k}} + (d-2)].
\end{aligned}
\tag{A5}
$$

We can then obtain the form of s_x by the function of the straight line:

$$
s_y = \frac{1}{2(d-1)}[\frac{d-(d-2)k}{\sqrt{k^2+1-\frac{2d-4}{d}k}} + (d-2)].
\tag{A6}
$$

It is interesting that (s_x, s_y) here is not directly relevant to the value of (r_x, r_y), but a function of its ratio k.

[1] N. Brunner, D. Cavalcanti, S. Pironio, V. Scarani, and S. Wehner, Bell nonlocality, Reviews of Modern Physics **86**, 419 (2014).

[2] P. Busch, P. Lahti, and R. F. Werner, Measurement uncertainty relations, Journal of Mathematical Physics **55**, 042111 (2014).

[3] H. P. Robertson, The uncertainty principle, Physical Review **34**, 163 (1929).

[4] Y.-C. Liang, R. W. Spekkens, and H. M. Wiseman, Specker's parable of the overprotective seer: A road to contextuality, nonlocality and complementarity, Physics Reports **506**, 1 (2011).

[5] M. Um, Q. Zhao, J. Zhang, P. Wang, Y. Wang, M. Qiao, H. Zhou, X. Ma, and K. Kim, Randomness expansion secured by quantum contextuality, Physical Review Applied **13**, 034077 (2020).

[6] R. Uola, A. C. Costa, H. C. Nguyen, and O. Gühne, Quantum steering, Reviews of Modern Physics **92**, 015001 (2020).

[7] P. Skrzypczyk, I. Šupić, and D. Cavalcanti, All sets ofincompatible measurements give an advantage in quantum state discrimination, Physical Review Letters **122**, 130403 (2019).

[8] H. M. Wiseman, S. J. Jones, and A. C. Doherty, Steering, entanglement, nonlocality, and the einstein-podolsky-rosen paradox, Physical Review Letters **98**, 140402 (2007).

[9] A. Fine, Hidden variables, joint probability, and the bell inequalities, Physical Review Letters **48**, 291 (1982).

[10] M. M. Wolf, D. Perez-Garcia, and C. Fernandez, Measurementsincompatible in quantum theory cannot be measured jointly in any other no-signaling theory, Physical Review Letters **103**, 230402 (2009).

[11] S.-L. Chen, C. Budroni, Y.-C. Liang, and Y.-N. Chen, Natural framework for device-independent quantification of quantum steerability, measurement incompatibility, and self-testing, Physical Review Letters **116**, 240401 (2016).

[12] C. Carmeli, T. Heinosaari, and A. Toigo, Quantum incompatibility witnesses, Physical Review Letters **122**, 130402 (2019).

[13] R. Uola, T. Kraft, J. Shang, X.-D. Yu, and O. Gühne, Quantifying quantum resources with conic programming, Physical Review Letters **122**, 130404 (2019).

[14] D. Wu, Q. Zhao, Y.-H. Luo, H.-S. Zhong, L.-C. Peng, K. Chen, P. Xue, L. Li, N.-L. Liu, C.-Y. Lu, *et al.*, Entanglement-free witnessing of quantum incompatibility in a high-dimensional system, Physical Review Research **3**, 023017 (2021).

[15] R. Uola, C. Budroni, O. Gühne, and J.-P. Pellonpää, One-to-one mapping between steering and joint measurability problems, Physical Review Letters **115**, 230402 (2015).

[16] P. Skrzypczyk and N. Linden, Robustness of measurement, discrimination games, and accessible information, Physical Review Letters **122**, 140403 (2019).

[17] G. Styliaris and P. Zanardi, Quantifying the incompatibility of quantum measurements relative to a basis, Physical Review Letters **123**, 070401 (2019).

[18] M. A. Ballester, S. Wehner, and A. Winter, State discrimination with post-measurement information, IEEE Transactions on Information Theory **54**, 4183 (2008).

[19] D. Gopal and S. Wehner, Using postmeasurement information in state discrimination, Physical Review A **82**, 022326 (2010).

[20] C. Carmeli, T. Heinosaari, and A. Toigo, State discrimination with postmeasurement information and incompatibility of quantum measurements, Physical Review A **98**, 012126 (2018).

[21] M. Piani and J. Watrous, Necessary and sufficient quantum information characterization of einstein-podolsky-rosen steering, Physical Review Letters **114**, 060404 (2015).

[22] C. Napoli, T. R. Bromley, M. Cianciaruso, M. Piani, N. Johnston, and G. Adesso, Robustness of coherence: an operational and observable measure of quantum coherence, Physical Review Letters **116**, 150502 (2016).

[23] R. Takagi, B. Regula, K. Bu, Z.-W. Liu, and G. Adesso, Operational advantage of quantum resources in subchannel discrimination, Physical Review Letters **122**, 140402 (2019).

[24] J. Bae, D. Chruściński, and M. Piani, More entanglement implies higher performance in channel discrimination tasks, Physical Review Letters **122**, 140404 (2019).

[25] W. K. Wootters and B. D. Fields, Optimal state-determination by mutually unbiased measurements, Annals of Physics **191**, 363 (1989).

[26] I. Ivonovic, Geometrical description of quantal state determination, Journal of Physics A: Mathematical and General **14**, 3241 (1981).

[27] R. Beneduci, T. J. Bullock, P. Busch, C. Carmeli, T. Heinosaari, and A. Toigo, Operational link between mutually unbiased bases and symmetric informationally complete positive operator-valued measures, Physical Review A **88**, 032312 (2013).

[28] C. Carmeli, T. Heinosaari, T. Miyadera, and A. Toigo, Witnessing incompatibility of quantum channels, Journal of Mathematical Physics **60**, 122202 (2019).

[29] S. Designolle, P. Skrzypczyk, F. Fröwis, and N. Brunner, Quantifying measurement incompatibility of mutually unbiased bases, Physical Review Letters **122**, 050402 (2019).

[30] C. Carmeli, T. Heinosaari, and A. Toigo, Informationally complete joint measurements on finite quantum systems, Physical Review A **85**, 012109 (2012).

[31] E. Chitambar and G. Gour, Quantum resource theories, Reviews of Modern Physics **91**, 025001 (2019).

[32] R. Uola, T. Moroder, and O. Gühne, Joint measurability of generalized measurements implies classicality, Physical Review Letters **113**, 160403 (2014).

[33] M. T. Quintino, T. Vértesi, and N. Brunner, Joint measurability, einstein-podolsky-rosen steering, and bell nonlocality, Physical Review Letters **113**, 160402 (2014).